Thermodynamics of Fluid Mixtures Near to and Far from the Critical Region

Leo Lue and John M. Prausnitz
Dept. of Chemical Engineering, University of California and
Chemical Sciences Div., Lawrence Berkeley National Laboratory, Berkeley, CA 94720

A theory for an equation of state for simple fluid mixtures valid both near to and far from critical points is presented. The base equation of state obtained from integral-equation theory using the mean-spherical approximation is used to compute the contribution of short-wavelength fluctuations to the free energy of the fluid mixture. Wilson's phase-space cell approximation, as extended by White, is used to compute the contribution of long-wavelength fluctuations. The resulting theory possesses nonclassic critical exponents similar to those observed experimentally. Far from the critical region, where long-wavelength fluctuations are not important, the theory reduces to that corresponding to the base equation of state. The complete theory is used to represent the thermodynamic properties and phase behavior of binary mixtures of methane, carbon dioxide, and n-butane. In the critical region, agreement with experiment is dramatically improved upon, adding to the base equation of state corrections from long-wavelength fluctuations.

Introduction

The thermodynamic properties of fluid mixtures are of much interest in chemical engineering, primarily for the design of separation operations. These properties are often provided through a phenomenological equation of state such as the Redlich-Kong-Soave or Peng-Robinson equations. By a suitable adjustment of the equation-of-state constants, these equations tend to perform fairly well far from the critical points of the fluids; however, they yield poor results near the critical point. While renormalization-group methods have been successful in describing the behavior of systems near critical points, much of the work in this area is only applicable to the region asymptotically close to the critical point.

For engineering applications it is desirable to have an equation of state that is accurate both near to and far from the critical point. One method for obtaining such an equation is to splice together the known behavior of fluids asymptotically close to the critical point, with an equation of state that works well far away from the critical region. An equation of state using this approach is typically referred to as a crossover equation of state as described for pure fluids (Chen et al., 1990; Kiselev, 1990; Kiselev et al., 1991; Kiselev and Sengers, 1993; Kiselev and Kostyukova, 1993). This approach has been extended to binary fluid mixtures of type I (Leung and Griffiths, 1973; Jin et al., 1993; Povodyrev et al., 1996; Kiselev, 1997), as well as other types of mixtures (Anisimov et al., 1995a,b, 1996; Cheng et al., 1997). Regrettably, several parameters are required to fit experimental data for each system.

Another method, known as hierarchical reference theory (Parola and Reatto, 1984, 1985; Meroni et al., 1990), is to reformulate liquid-state theory to take into account density fluctuations on successively larger length scales. This method has been applied to Lennard-Jones fluids and to fluids with three-body interactions (Meroni et al., 1993). The hierarchical reference theory has also been extended to fluid mixtures (Parola and Reatto, 1991, 1993). However, because this method is computationally intensive, it is not suitable for typical engineering applications.

Wilson (1971a,b) introduced the phase-space cell approximation for the semiquantitative analysis of the behavior of systems near the critical point. This procedure yields (Wilson, 1971b; Wilson and Fisher, 1972; Grover, 1972; Grover et al., 1972; Salvino and White, 1992) an equation of state with nonclassic exponents close to those observed experimentally (Sengers, 1991). Table 1 compares nonclassic and classic exponents obtained by commonly used analytical equations of

---

Correspondence concerning this article should be addressed to J. M. Prausnitz.
Present address of L. Lue: Physical and Chemical Properties Division, 838.08, National Institute of Standards and Technology, 325 Broadway, Boulder, CO 80303.

Table 1. Critical Exponents for a Simple Fluid

	β	γ	δ	ν	η
Expt.*	0.32–0.39	1.3–1.4	4–5	0.6–0.7	0.1
Classic	0.5	1	3	0.5	0
Wilson and this work	0.34**	1.22†	4.8**	0.61†	0†

*From Sengers (1991).
**From Salvino and White (1992).
†From Wilson (1971b).

state. The phase-space cell approximation yields the exact (Wilson and Fisher, 1972) critical exponents to first order in the $\epsilon = 4 - D$ expansion (where D is the dimension of space) and gives the exact exponents for the n-component spin model in the limit when the number of spin components approaches infinity (Ma, 1976).

White and coworkers (Salvino and White, 1992; White and Zhang, 1993, 1995, 1997) extended the range of applicability of the phase-space cell approximation to regions of the phase diagram beyond the critical regime. The resulting theory is computationally efficient and agrees well with experimental data for the equation of state in a broad region around the critical point for various pure fluids. Recently, this method has been extended to a larger region around the critical point (White and Zhang, 1997; Lue and Prausnitz, 1998).

In this work we extend this method to multicomponent fluids. First, we recast the partition function in terms of a functional integral. In addition, we discuss how different approximations to the functional integral lead to various well-known models of fluids. We present the basic ideas of the approximate renormalization method. We discuss our implementation of White's global renormalization scheme to fluids. To illustrate its engineering utility, we apply the theory to binary fluid mixtures of methane, carbon dioxide, and n-butane. Finally, we summarize our findings and give some concluding remarks.

Field Theory for Simple Fluids

Consider an open multicomponent system consisting of ω components at absolute temperature, T, species chemical potential, μ_α, and total volume, V. We specify that the fluid's molecules interact with a spherically symmetric pair potential, $u_{\alpha\gamma}(r)$; further, each of the molecules interacts with an external field, $e_\alpha(r)$. The grand partition function, Ξ, of this system is given by (Hansen and McDonald, 1986)

$$\Xi = \sum_{N_1=0}^{\infty} \cdots \sum_{N_\omega=0}^{\infty} \prod_{\sigma} \frac{\exp(\beta\mu_\sigma N_\sigma)}{N_\sigma!\Lambda_\sigma^{3N}} \times \int \sum_{\tau t} d^3 r_{\tau t} \exp\left\{-\frac{\beta}{2}\sum_{\alpha j \neq \gamma k} u_{\alpha\gamma}(r_{\alpha j} - r_{\gamma k}) - \beta \sum_{\alpha j} e_\alpha(r_{\alpha j})\right\}, \tag{1}$$

where r is the center-to-center distance between molecules; $\beta = 1/(k_B T)$; k_B is the Boltzmann constant; N_σ is the number of particles of type σ; $r_{\alpha j}$ is the position of the jth molecule of type α; and Λ_σ is the thermal wavelength of a molecule of type σ.

We divide the interaction potential, $u_{\alpha\gamma}(r)$, into a reference contribution, $u_{\alpha\gamma}^{\mathrm{ref}}(r)$, due mainly to repulsive interactions, and a perturbative contribution, $u'_{\alpha\gamma}(r)$, due mainly to attractive interactions [i.e., $u_{\alpha\gamma}(r) = u_{\alpha\gamma}^{\mathrm{ref}}(r) + u'_{\alpha\gamma}(r)$]. The grand partition function can be rewritten (Negele and Orland, 1988)

$$\Xi[\boldsymbol{\nu}] = \int \prod_{\sigma} \mathfrak{D}\rho_\sigma(\cdot)\, \mathfrak{D}\phi_\sigma(\cdot) \exp\left\{-\frac{1}{2}\sum_{\alpha\gamma} \int d^3r d^3r' \rho_\alpha(r) \upsilon_{\alpha\gamma} \times (r - r')\rho_\gamma(r') + \sum_{\alpha} \int d^3 r \rho_\alpha(r) \nu_\alpha(r) - i \sum_{\alpha} \int d^3 r \rho_\alpha(r) \phi_\alpha(r) + \ln \Xi^{\mathrm{ref}}[i\boldsymbol{\phi}]\right\}, \tag{2}$$

where $i = \sqrt{-1}$; $\nu_\alpha(r) = \beta[\mu_\alpha - e_\alpha(r)]$; $\upsilon_{\alpha\gamma}(r) = \beta u'_{\alpha\gamma}(r)$; and Ξ^{ref} is the grand partition function for the reference fluid;

$$\Xi^{\mathrm{ref}}[\boldsymbol{\nu}] = \sum_{N_1=0}^{\infty} \cdots \sum_{N_\omega=0}^{\infty} \prod_{\sigma} \frac{1}{N_\sigma!\Lambda_\sigma^{3N}} \times \int \prod_{\tau t} d^3 r_{\tau t} \exp\left\{-\frac{\beta}{2}\sum_{\alpha j \neq \gamma k} u_{\alpha\gamma}^{\mathrm{ref}}(r_{\alpha j} - r_{\gamma k}) + \sum_{\alpha j} \nu_\alpha(r_{\alpha j})\right\}. \tag{3}$$

The boldface indicates a particular property for all components. For example, $\boldsymbol{\nu}$ represents the set $\{\nu_1, \nu_2, \ldots, \nu_\omega\}$. In Eq. 2, the symbol $\int \prod_\sigma \mathfrak{D}\rho_\sigma(\cdot)\, \mathfrak{D}\phi_\sigma(\cdot)$ indicates a *functional* integration, where $\rho_\sigma(r)$ and $\phi_\sigma(r)$ are the integration variables, and the range of integration is over all possible "shapes" of these functions. The function $\rho_\sigma(r)$ can be interpreted as the instantaneous density distribution of molecules of type σ in the system; the function $\phi_\sigma(r)$ can be interpreted as a potential field felt by molecules of type σ that is generated by the perturbation potential of all the molecules in the system.

For all but a few oversimplified interaction potentials, approximations are needed to evaluate the functional integral in Eq. 2. If the saddle-point method (Negele and Orland, 1988) is used to approximate the value of the functional integral, the Helmholtz energy per unit volume of the system, f, becomes

$$f = f^{\mathrm{ref}} - \sum_{\alpha\gamma} a_{\alpha\gamma} \rho_\alpha \rho_\gamma, \tag{4}$$

where f^{ref} is the Helmholtz energy per unit volume for the reference system; ρ_α is the density of component α in the fluid; and $a_{\alpha\gamma}$ is the interaction volume between molecules of types α and γ, given by

$$a_{\alpha\gamma} = -\frac{1}{2}\int d^3 r u'_{\alpha\gamma}(r). \tag{5}$$

Equation 4 has the form of the classic van der Waals equation. The saddle-point approximation neglects the contribution of density fluctuations of all wavelengths that are not already accounted for by the reference system.

We can add fluctuation corrections to the saddle-point approximation by expanding the exponent of the integrand of the functional integral in Eq. 2 in a Taylor series in the fields, ϕ_α, and neglecting terms higher than second order. The resulting functional integral can be performed analytically. This approximation, also known as the Gaussian approximation, yields (Negele and Orland, 1988):

$$f = f^{\mathrm{ref}} + \frac{1}{2}\int \frac{d^3q}{(2\pi)^3} \ln\det\left[1 + \hat{v}(q)\hat{\chi}^{\mathrm{ref}}(q)\right], \tag{6}$$

where

$$\hat{\chi}^{\mathrm{ref}}_{\alpha\gamma}(q) = \rho_\alpha \delta_{\alpha\gamma} + \rho_\alpha \hat{h}^{\mathrm{ref}}_{\alpha\gamma}(q)\rho_\gamma. \tag{7}$$

Here $h^{\mathrm{ref}}_{\alpha\gamma}$ is the total correlation function between components α and γ in the reference fluid. The symbol ^ denotes the three-dimensional Fourier transform of a function. Equation 6 is the well-known random-phase approximation (RPA) (Andersen and Chandler, 1970; Chandler and Andersen, 1971). If the reduced perturbation potential, $v_{\alpha\gamma}(r)$, is chosen such that the pair-correlation function is equal to zero inside the hard core, the RPA becomes the optimized random-phase approximation (ORPA) (Andersen and Chandler, 1972).

Several "conventional" theories adequately describe the behavior of fluids far from the critical region. These include the cubic equations of state based on the mean-field approximation, liquid-state theories based on integral-equation theory such as the hypernetted-chain equation, the mean-spherical approximation, and perturbation theories.

Far from the critical point, the correlation length, ξ, is small, on the order of magnitude of molecular dimensions. For distances exceeding ξ, molecules in the fluid are essentially uncorrelated. Conventional theories perform well in this regime because ξ is small; only correlations between a few particles contribute significantly to the free energy.

However, as the critical point is approached, the correlation length increases, diverging to infinity. An increasing correlation length means that correlations between larger and larger numbers of molecules make an increasingly significant contribution to the properties of the system. Most of the common approximations in liquid-state theories are not adequate to accurately describe correlations between large numbers of molecules: therefore, they perform poorly in the critical region.

As discussed by Sengers (1991), neglect of long-wavelength fluctuations results in a theoretical free energy that is analytic at the critical point, and therefore does not show the correct behavior in the critical regime. To include long-wavelength fluctuations, Wilson (1971a,b) constructed an approximate renormalization-group method.

Long-Wavelength-Fluctuation Corrections

The first step toward including the contribution of long-wavelength fluctuations to the free energy is to divide the free energy into two parts: a short-wavelength contribution that can be described satisfactorily using conventional liquid-state theory, and a long-wavelength contribution that must be computed using a renormalization-group method.

We divide the reduced attractive interaction potential into a short-wavelength, $v^{(s)}_{\alpha\gamma}$, and long-wavelength contribution, $v^{(l)}_{\alpha\gamma}$ (Ivanchenko and Lisyansky, 1992, 1995; Ivanchenko et al., 1992).

$$\hat{v}^{-1}_{\alpha\gamma}(q) = [\hat{v}^{(s)}]^{-1}_{\alpha\gamma}(q) - [\hat{v}^{(l)}]^{-1}_{\alpha\gamma}(q) \tag{8}$$

The definitions of $v^{(s)}_{\alpha\gamma}$ and $v^{(l)}_{\alpha\gamma}$ are arbitrary, provided $[\hat{v}^{(s)}]^{-1}_{\alpha\gamma}(q)$ rapidly approaches $\hat{v}^{-1}_{\alpha\gamma}(q)$ when $q > 2\pi/L$, and $[\hat{v}^{(l)}]^{-1}_{\alpha\gamma}(q)$ rapidly approaches $\hat{v}^{-1}_{\alpha\gamma}(q)$ when $q < 2\pi/L$. The length L is chosen such that contributions from fluctuations of length scales less than L can be adequately calculated by standard approximation methods, such as the Gaussian approximation.

We choose the following form for the long-wavelength interaction potential

$$\hat{v}^{(l)}_{\alpha\gamma}(q) = -2\beta a_{\alpha\gamma} + q^2\beta a_{\alpha\gamma}\zeta^2_{\alpha\gamma}, \tag{9}$$

where $a_{\alpha\gamma}$ is given in Eq. 5, and $\zeta_{\alpha\gamma}$ denotes the range of the attractive interaction potential

$$a_{\alpha\gamma}\zeta^2_{\alpha\gamma} = -\frac{1}{3!}\int d^3r r^2 u'_{\alpha\gamma}(r). \tag{10}$$

With the division of the perturbation interaction potential into two parts, we can divide (Ivanchenko and Lisyansky, 1992, 1995; Ivanchenko et al., 1992) the density field, $\rho_\alpha(r)$, into two contributions: $\rho^{(l)}_\alpha$, which consists primarily of long-wavelength components (i.e., wavelengths greater than L), and $\rho^{(s)}_\alpha$, which consists primarily of short-wavelength components (i.e., wavelengths shorter than L). Introducing these new variables into the partition function (see Eq. 2), we find

$$\Xi = \frac{1}{Q^{(l)}}\int \prod_\sigma \mathfrak{D}\rho^{(l)}_\sigma(\cdot)\exp\left\{-\frac{1}{2}\sum_{\alpha\gamma}\int d^3r d^3r' \rho^{(l)}_\alpha(r) v^{(l)}_{\alpha\gamma}(r-r') \times \rho^{(l)}_\alpha(r') + \sum_\alpha \int d^3r \rho^{(l)}_\alpha(r)\nu_\alpha(r) - \mathfrak{F}^{(s)}[\boldsymbol{\rho}^{(l)}]\right\}, \tag{11}$$

where

$$\exp\{-\mathfrak{F}^{(s)}[\boldsymbol{\rho}^{(l)}]\} = \frac{Q}{Q^{(s)}}\int \prod_\sigma \mathfrak{D}\rho^{(s)}_\sigma(\cdot)\,\mathfrak{D}\phi_\sigma(\cdot) \exp\left\{-\frac{1}{2}\sum_{\alpha\gamma}\int d^3r d^3r' \rho^{(s)}_\alpha(r) v^{(s)}_{\alpha\gamma}(r-r')\rho^{(s)}_\gamma(r') + \sum_\alpha \int d^3r \rho^{(s)}_\alpha(r)\nu_\alpha(r) - i\sum_\alpha \int d^3r\left[\rho^{(l)}_\alpha(r) + \rho^{(s)}_\alpha(r)\right]\phi_\alpha(r) + \ln \Xi^{\mathrm{ref}}[i\boldsymbol{\phi}]\right\} \tag{12}$$

$$Q = \int \prod_\sigma \mathfrak{D}\rho_\sigma(\cdot)\exp\left\{-\frac{1}{2}\int d^3r d^3r' \rho_\alpha(r) v_{\alpha\gamma}(r-r')\rho_\gamma(r')\right\} \tag{13}$$

$$Q^{(l)} = \int \prod_{\sigma} \mathfrak{D}\rho_{\sigma}(\cdot)\exp\left\{ -\frac{1}{2}\int d^3r d^3r' \rho_{\alpha}(r) v_{\alpha\gamma}^{(l)}(r-r')\rho_{\gamma}(r')\right\} \tag{14}$$

$$Q^{(s)} = \int \prod_{\sigma} \mathfrak{D}\rho_{\sigma}(\cdot)\exp\left\{ -\frac{1}{2}\int d^3r d^3r' \rho_{\alpha}(r) v_{\alpha\gamma}^{(s)}(r-r')\rho_{\gamma}(r')\right\}. \tag{15}$$

Density profiles $\rho_{\alpha}^{(l)}(r)$ have no small-wavelength components. The functional $\mathfrak{F}^{(s)}$ accounts for short-wavelength fluctuations but not for long-wavelength fluctuations.

To evaluate $\mathfrak{F}^{(s)}$, we need to make further approximations. We introduce the local-density approximation,

$$\mathfrak{F}^{(s)}[\boldsymbol{\rho}] \approx \int d^3r f^{(s)}(\boldsymbol{\rho}(r)), \tag{16}$$

where $f^{(s)}$ is the free energy per unit volume for a uniform system.

If we completely neglect the contribution of the short-wavelength portion of the attraction potential (i.e., if we choose $[\hat{v}^{(s)}]_{\alpha\gamma}^{-1}(q) = 0$), we find

$$f^{(s)} \approx f^{\text{ref}}. \tag{17}$$

This is the form White and coworkers used in their analysis.

To obtain a better description of the fluid, we need to consider $f^{(s)}$ more carefully. The short-wavelength response of a fluid is governed primarily by the repulsive part of its interaction potential (Weeks et al., 1971), that is, for $qd > \pi$, $\hat{h}(q) \approx \hat{h}^{\text{ref}}(q)$, where d is the diameter of the repulsive core of a molecule in the fluid. When only short-wavelength fluctuations contribute significantly to the free energy, standard liquid-state theories, such as the mean spherical approximation (MSA), work well. This suggests that we should use a liquid-state free-energy model, like that of the MSA, f^{MSA}, as an approximation for $f^{(s)}$. However, while the function $f^{(s)}$ accounts only for short-wavelength fluctuations, f^{MSA} includes both short and long-wavelength fluctuations, although the long-wavelength fluctuations are given crudely. Therefore, before we add contributions from long-wavelength fluctuations calculated from renormalization methods, we need to subtract the MSA's estimate for the contribution of long-wavelength fluctuations. To do so, we choose the following form

$$f^{(s)} = f^{\text{MSA}} + \sum_{\alpha\gamma} a_{\alpha\gamma}\rho_{\alpha}\rho_{\gamma}. \tag{18}$$

The second term, $\sum_{\alpha\gamma} a_{\alpha\gamma}\rho_{\alpha}\rho_{\gamma}$, in Eq. 18 subtracts the long-wavelength contributions provided by the MSA. However, Eq. 18 gives only a crude approximation, because the second term in the equation only subtracts the $q = 0$ contribution, $-\sum_{\alpha\gamma} a_{\alpha\gamma}\rho_{\alpha}\rho_{\gamma}$. Therefore, in addition, it is necessary also to subtract the contributions from fluctuations of other wave numbers $q < 2\pi/L$.

Substituting Eq. 16 into the functional integral in Eq. 11 yields

$$\Xi[\boldsymbol{\nu}] = \frac{1}{Q^{(l)}}\int \prod_{\sigma} \mathfrak{D}\rho_{\sigma}^{(l)}(\cdot)\exp\{-\beta\mathcal{H}^{(l)}[\boldsymbol{\rho}^{(l)}]\}, \tag{19}$$

where the Hamiltonian, $\mathcal{H}$, is given by

$$\mathcal{H}^{(l)}[\boldsymbol{\rho}^{(l)}] = \sum_{\alpha\gamma}\frac{a_{\alpha\gamma}\zeta_{\alpha\gamma}^2}{2}\int d^3r \nabla\rho_{\alpha}^{(l)}(r)\cdot\nabla\rho_{\gamma}^{(l)}(r) + \int d^3r\left[f^{(s)}(\boldsymbol{\rho}^{(l)}(r)) - \sum_{\alpha\gamma} a_{\alpha\gamma}\rho_{\alpha}^{(l)}(r)\rho_{\gamma}^{(l)}(r)\right]. \tag{20}$$

In general, a Hamiltonian, $\mathcal{H}$, relates the energy of the system to the density distributions of the various components in the system. To obtain the partition function, Ξ, from the Hamiltonian, one must integrate over all possible shapes of the functions $\rho_{\alpha}(r)$. However, the integration in Eq. 19 is restricted to density distributions, $\rho_{\alpha}^{(l)}(r)$, which are smooth on length scales less than L. Over distances less than L, $\rho_{\alpha}^{(l)}(r)$ should be nearly constant because those portions of the density profiles that are not smooth were already integrated when the variables $\rho_{\alpha}^{(s)}(r)$ were integrated to obtain $\mathfrak{F}^{(s)}$. Therefore, $\mathcal{H}^{(l)}$ is a partially integrated version of $\mathcal{H}$ in which fluctuations of wavelengths less than L have been "averaged out." This process can be thought of as dividing the fluid into several boxes of volume L^3. Within each box, we microscopically average over all the properties. The density distributions, $\rho_{\alpha}^{(l)}(r)$, are the average density inside each box, because the small-wavelength variations of the actual density profile, $\rho_{\alpha}(r)$, inside each box have been averaged by integrating over $\rho_{\alpha}^{(s)}(r)$.

If $L \gg \xi$, different boxes are essentially decoupled from each other, and the functional integral in Eq. 19 can be factored and easily evaluated. The free energy of the entire system is the sum of the free energies of each box in the system. The second term in Eq. 20 represents the sum of the free energies of each box, and the free energy of the entire system is the integrand of the second term.

However, if $L < \xi$, the situation is different. In this case, boxes that are separated by less than distance ξ are significantly coupled with each other. We can no longer write the free energy as a simple sum of the free energies of all boxes because the boxes interact with each other. The first term in Eq. 20 represents the contribution of these interactions. The functional integral in Eq. 19 is no longer easy to evaluate. As indicated earlier, one method to evaluate the functional integral in Eq. 19 is the saddle-point approximation. This yields

$$f^{(0)} = f^{(s)}(\boldsymbol{\rho}^{(l)}(r)) - \sum_{\alpha\gamma} a_{\alpha\gamma}\rho_{\alpha}^{(l)}(r)\rho_{\gamma}^{(l)}(r), \tag{21}$$

where superscript (0) denotes that $f^{(0)}$ is a "zeroth"-order approximation to f. This approximation neglects the effect of fluctuations of wavenumbers $0 < q < 2\pi/L$. The fluctuations of wavenumbers $q > 2\pi/L$ are accounted for by $f^{(s)}$. When $L \gg \xi$, the saddle-point approximation becomes highly accurate. In our approximation for $f^{(s)}$ (see Eq. 18), Eq. 21 reduces to the mean-spherical approximation.

A strategy to incorporate fluctuations with wavelengths greater than L (important when $L < \xi$) is gradually to integrate over larger and larger length scales, starting at L, until we are averaging over length scales much larger than ξ. That is, we want to evaluate the following integral

$$\exp\{-\beta \mathcal{H}^{(l')}[\boldsymbol{\rho}^{(l')}]\} = \frac{1}{\mathfrak{N}} \int \mathfrak{D}\bar{\rho}^{(l)} \cdot \exp\{-\beta \mathcal{H}^{(l)}[\boldsymbol{\rho}^{(l)}]\}, \tag{22}$$

where $\rho^{(l')}$ represents density profiles that are smooth on length scales $L' > L$; $\mathcal{H}^{(l')}$ is a Hamiltonian for these density profiles; and $\mathfrak{N}$ is a normalization constant. The integration variable $\boldsymbol{\rho}^{(l)}$ represents variations of $\rho^{(l)}$ between length scales L and L'. That is, we integrate over all density fluctuations of length scales between L and L'.

Equation 22 can be used iteratively to integrate over larger and larger length scales. As we integrate over larger and larger length scales, the Hamiltonian, $\mathcal{H}^{(l)}$, gradually changes, or is renormalized. Eventually, when L, the length scale for averaging, is much greater than the correlation length, ξ, the Hamiltonian does not change anymore. The interaction term gradually becomes smaller and smaller until it disappears completely. The free energy of the fluid can then be obtained from the saddle-point approximation, which is accurate at these conditions.

The integral in Eq. 22 cannot be performed analytically and is, in fact, as difficult to evaluate as the integral in Eq. 2. Approximation methods must be used to evaluate the integral. However, the advantage of making approximations to the integral in Eq. 22 is that long-wavelength fluctuations are taken into account in a much more satisfactory manner, leading to nonclassic critical exponents. In the next section, we discuss one method to evaluate this integral, known as the phase-space cell approximation.

Phase-Space Cell Approximation

As longer and longer wavelength fluctuations are incorporated into the theory, the free energy gradually changes. The phase-space cell approximations lead to the following recursion relations that specify how the free energy changes as fluctuation effects are added.

$$\begin{aligned} f^{(n)}(\boldsymbol{\rho}) &= f^{(n-1)}(\boldsymbol{\rho}) + \delta f^{(n)}(\boldsymbol{\rho}) \\ \delta f^{(n)}(\boldsymbol{\rho}) &= -\frac{k_B T}{(2^n L)^3} \ln \frac{I_{n,s}(\boldsymbol{\rho})}{I_{n,l}(\boldsymbol{\rho})} \quad \text{for } 0 \le \rho < \rho_{\max}/2 \\ \delta f^{(n)}(\boldsymbol{\rho}) &= 0 \qquad \text{for } \rho_{\max}/2 \le \rho < \rho_{\max}, \end{aligned} \tag{23}$$

where $\rho = \sum_\sigma \rho_\sigma$ is the total density of molecules in the system, $\rho_{\max}$ is the maximum possible density of molecules in the system, and

$$K_n = \frac{k_B T}{(2^n L)^3} \tag{24}$$

$$I_{n,i}(\boldsymbol{\rho}) = \int_0^{\rho_1} dx_1 \int_0^{\rho_2} dx_2 \cdots \int_0^{\rho_\omega} dx_\omega \exp[-G_{n,i}(\boldsymbol{\rho}, \boldsymbol{x})/K_n] \qquad i = s, l \tag{25}$$

$$2G_{n,i}(\boldsymbol{\rho}, \boldsymbol{x}) = \bar{f}_{n,i}(\boldsymbol{\rho} + \boldsymbol{x}) + \bar{f}_{n,i}(\boldsymbol{\rho} - \boldsymbol{x}) - 2\bar{f}_{n,i}(\boldsymbol{\rho}) \qquad i = s, l \tag{26}$$

$$\bar{f}_{n,l}(\boldsymbol{\rho}) = f^{(n-1)}(\boldsymbol{\rho}) + \sum_{\alpha\gamma} a_{\alpha\gamma} \rho_\alpha \rho_\gamma \tag{27}$$

$$\bar{f}_{n,s}(\boldsymbol{\rho}) = f^{(n-1)}(\boldsymbol{\rho}) + \sum_{\alpha\gamma} a_{\alpha\gamma} \Delta_{\alpha\gamma} \left(\frac{\zeta_{\alpha\gamma}}{2^n L} \right)^2 \rho_\alpha \rho_\gamma . \tag{28}$$

A derivation of this recursion relation is given in the Appendix: it is based closely on the work of Wilson (1971b), White and Zhang (1995), and Battle (1994). The density fluctuations are written as an expansion in basis functions generated by translations and dilations of a single wavelet function, ψ_α (see Appendix and Battle (1994) for details). Parameter $\Delta_{\alpha\gamma}$ is the average gradient of the wavelet, that is,

$$\int d^3 r \nabla \psi_\alpha(r) \cdot \nabla \psi_\gamma(r) = \Delta_{\alpha\gamma} . \tag{29}$$

This average gradient should depend only on the particular wavelet functions, ψ_α, chosen and not on the potential function. These parameters are adjusted to fit experimental critical data.

In our work, the initial approximation for the Helmholtz energy per unit volume, $f^{(0)}$, is given by Eq. 21. It is assumed that fluctuations with wavelengths less than L are well accounted for by $f^{(0)}$. In this work, we choose $L = 5.10$ Å.

To include long-wavelength fluctuations in the free-energy model, we begin with an approximation for $f^{(0)}$ (e.g., Eq. 21). The free energy $f^{(0)}$ neglects fluctuations of wave number $0 < q < 2\pi/L$. By inserting $f^{(0)}$ into the recursion relations, Eqs. 23–28, we obtain successive approximations to the Helmholtz free energy per unit volume, $f^{(n)}$, each containing the contribution of fluctuations of larger and larger wavelengths. The free energy $f^{(n)}$ contains fluctuation contributions from wavenumbers $0 < q < 2\pi/(2^n L)$. In principle, we should use $f^{(\infty)}$ as our final free energy. In practice, the free energies are nearly identical for $n > 5$; therefore, we use $f^{(5)}$ as our "final" free energy.

The calculations in the recursion relations must be performed numerically. The initial free energy is computed on a density grid with spacing $\Delta \rho_\alpha = 0.0025(6/\pi d_\alpha^3)$ for each component α, where d_α is the hard-sphere diameter of component α. The integral in Eq. 25 is performed using the trapezoid rule. The final free energy is fit using a piecewise-smooth cubic spline; the pressure and chemical potential were computed from the free energy using derivatives of the spline fit. A computer program that renormalizes the free energy according to the recursion relations is available upon request from the authors.

Application to Single-Component Systems

For interactions between molecules we use the square-well potential. The reference potential is a hard-sphere potential, given by

$$u^{\text{ref}}(r) = \begin{cases} \infty & r < d \\ 0 & r > d, \end{cases} \tag{30}$$

where d is the diameter of the repulsive interaction. The perturbation potential is

$$u'(r) = \begin{cases} -\epsilon & r < \lambda d \\ 0 & r > \lambda d, \end{cases} \tag{31}$$

where ϵ is the depth of the attractive potential, and λ is a constant related to the range of the attraction.

For this potential, parameters a and ζ (see Eqs. 5 and 10) are given by

$$a = \frac{2\pi}{3}\epsilon\lambda^3 d^3 \tag{32}$$

$$\zeta^2 = \frac{1}{5}\lambda^2 d^2. \tag{33}$$

The Helmholtz energy per unit volume, f, is written in the form

$$f = f^{\text{ref}} - \rho^2 \epsilon b \mathfrak{F}(k_B T \text{ divided by } \epsilon, \eta, \lambda), \tag{34}$$

where $b = \pi d^3/6$ is the volume of a molecule; $\eta = \rho b$ is the packing fraction of spheres in the system; and f^{ref} is the Helmholtz energy per unit volume of the reference fluid. The reference system is a hard-sphere fluid with diameter d. The properties of the reference system are given by the Carnahan-Starling (1969) equation of state. The formula for $\mathfrak{F}$ is too lengthy to reproduce here; it is given in Eqs. 13, 15, and 16 in Tang and Lu (1994).

To describe the properties of real fluids, we fit the square-well fluid interaction parameters, ϵ and d, to selected experimental data at fixed λ. Because the MSA accurately describes the properties of a fluid away from the critical point, we fit the interaction parameters to experimental liquid-phase densities and vapor pressures for temperatures 20% below the critical temperature, and to experimental density (PVT) data for temperatures 20% above the critical temperature. We obtained parameters for methane, carbon dioxide, and n-butane. Experimental data for pure methane are from Vargaftik (1975) and Kleinrahm and Wagner (1986); data for carbon dioxide are from Vargaftik (1975); data for n-butane are from Younglove and Ely (1987). Parameter $\Delta_{\alpha\alpha}$ was chosen to reproduce the experimentally observed critical temperature. The parameter λ was chosen to yield the correct critical pressure after the fluctuation corrections had been applied.

To achieve a satisfactory fit for carbon dioxide and n-butane, we need a temperature-dependent well depth, ϵ. We choose the following form

$$\epsilon = \epsilon^{(0)} + \frac{\epsilon^{(1)}}{T^2}. \tag{35}$$

Parameters for methane, carbon dioxide, and n-butane are given in Table 2.

Lue and Prausnitz (1998) compare predictions of the MSA and the MSA with renormalization-group corrections (MSA + RG) with experimental data for vapor–liquid coexistence curves, vapor–pressure curves, and pressure–density isotherms for these pure fluids. The comparison shows that the RG correction very much improves agreement with experiment in the critical region.

Table 2. Fitted Square-Well Parameters for Three Fluids when $L = 5.10$ Å

	Methane ($\Delta = 12.0$)	Carbon Dioxide ($\Delta = 9.15$)	n-Butane ($\Delta = 10.6$)
$\epsilon^{(0)}$ (MJ/mol)	8.75×10^{-4}	1.62×10^{-3}	2.26×10^{-3}
$\epsilon^{(1)}$ (MJ/mol·K^2)	—	4.92	13.4
σ (Å)	3.53	3.48	4.86
λ	1.75	1.65	1.65

Application to Fluid Mixtures

The mean-spherical approximation can be extended to multicomponent systems. In addition, the perturbative-solution method has been extended (Tang and Lu, 1995) to mixtures. However, the resulting formulas are cumbersome and the computation time required for evaluation rises dramatically with the number of components. Therefore, to simplify calculations, we approximate the Helmholtz energy per unit volume of the mixture, f, as

$$f = f^{\text{ref}} - \sum_{\alpha\gamma} \rho_\alpha \rho_{\alpha\gamma} \epsilon_\gamma b_{\alpha\gamma} \mathfrak{F}(k_B T/\epsilon_{\alpha\gamma}, \eta, \lambda_{\alpha\gamma}), \tag{36}$$

where $b_{\alpha\gamma} = \pi d_{\alpha\gamma}/6$, and $\eta = \sum_\alpha \rho_\alpha b_{\alpha\alpha}$. The reference system is an additive hard-sphere fluid with diameters d_α. The properties of the reference fluid are given by the Mansoori-Carnahan-Starling-Leland (1971) equation of state.

The square-well interaction parameters between unlike species are obtained from the parameters between like species by

$$\epsilon_{\alpha\gamma} = \sqrt{\epsilon_\alpha \epsilon_\gamma}(1 - k_{\alpha\gamma}) \tag{37}$$

$$d_{\alpha\gamma} = \frac{1}{2}(d_\alpha + d_\gamma) \tag{38}$$

$$\lambda_{\alpha\gamma} = \frac{1}{2}(\lambda_\alpha + \lambda_\gamma). \tag{39}$$

The single binary parameter $k_{\alpha\gamma}$ is fit to equation-of-state data for temperatures greater than 20% of the higher critical temperature and to mixture phase-equilibrium data with less than 0.1 mole fraction of the component with the higher critical temperature in the liquid phase for temperatures lower than 20% of the higher critical temperature.

Vapor–liquid phase-coexistence data for carbon dioxide/n-butane mixtures are from Olds et al. (1949), Nagahama et al. (1974), Kalra et al. (1976), Brown et al. (1989), Pozo de Fernandez et al. (1989), Shibata and Sandler (1989), Traub and Stephan (1990), and Weber (1989); data for methane/carbon dioxide mixtures are from Reamer et al. (1944), Arai et al. (1971), Davalos et al. (1976), Hwang et al. (1976), Mraw et al. (1978), Al-Sahhaf et al. (1983), Somait and Kidnay (1983), Xu et al. (1992), and Bian et al. (1993): data for methane/n-butane mixtures are from Sage et al. (1940), Roberts et al. (1962), Chen et al. (1974), Elliot et al.

Table 3. Binary Parameters for Binary Mixtures of Methane, Carbon Dioxide, and *n*-Butane

	k_{12}	Δ_{12}
Carbon dioxide/*n*-butane	0.185	17.6
Methane/carbon dioxide	0.0747	25.6
Methane/*n*-butane	0.0995	17.9

(1974), and Kahre (1974). Equation-of-state data for carbon dioxide/*n*-butane mixtures are from Olds et al. (1949); data for methane/carbon dioxide mixtures are from Reamer et al. (1944); data for methane/*n*-butane mixtures are from Reamer et al. (1947).

After fitting the parameter k_{12}, the parameter Δ_{12} is adjusted to give a reasonable fit to a pressure-composition envelope at a particular temperature. Table 3 gives these parameters for each of the mixtures studied here. Critical coordinates for the mixtures are not used as input data.

Figures 1, 2 and 3 show pressure-composition envelopes for carbon dioxide/*n*-butane, methane/carbon dioxide, and methane/*n*-butane mixtures, respectively. The symbols are experimental data; the dashed lines are predictions of the MSA; and the solid lines are results of the MSA with renormalization-group (MSA + RG) corrections. The MSA predicts a much larger two-phase envelope than that observed experimentally. The MSA + RG predictions are in much better agreement with experimental data. Far from the critical region of the fluid mixture, the predictions of the MSA and the MSA + RG coincide. The predictions of the MSA + RG can be adjusted by changing parameter Δ_{12}. Decreasing Δ_{12} decreases the two-phase region.

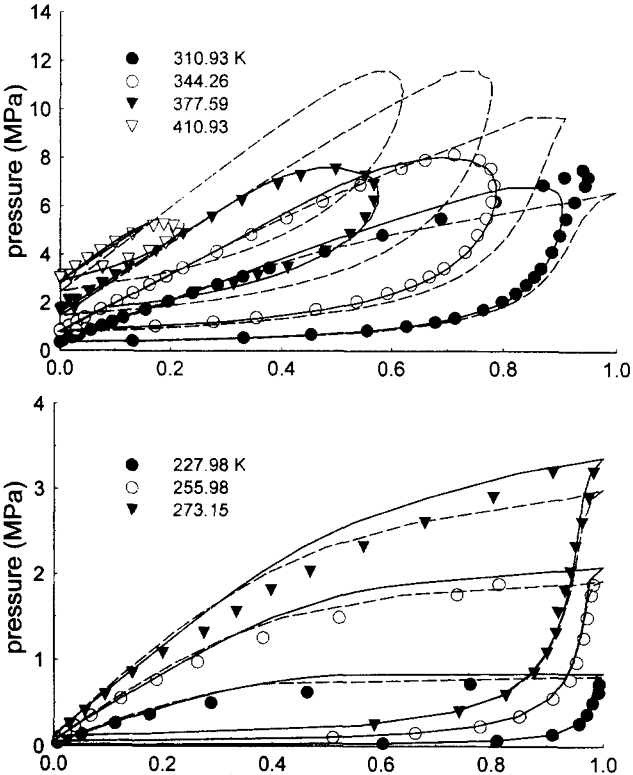

Figure 1. Pressure-composition envelopes for carbon dioxide/*n*-butane mixtures.

(1) Experimental data (symbols); (2) mean-spherical approximation (dashed lines); and (3) mean-spherical approximation with renormalization corrections (solid lines) (experimental data from Olds et al. (1949)).

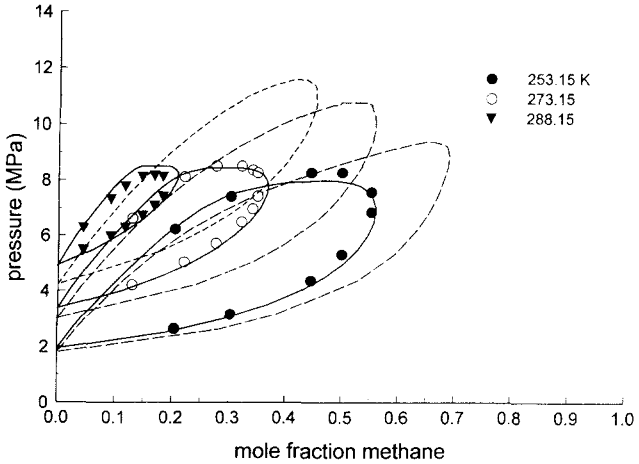

Figure 2. Pressure-composition envelopes for methane/carbon dioxide mixtures.

(1) Experimental data (symbols); (2) mean-spherical approximation (dashed lines); and (3) mean-spherical approximation with renormalization corrections (solid lines) (experimental data from Arai et al. (1971)).

Figure 4 shows the variation of phase densities with pressure for carbon dioxide/*n*-butane, methane/carbon dioxide, and methane/*n*-butane mixtures, respectively. The symbols are experimental data; the dashed lines are predictions of the MSA; and the solid lines show results of the MSA + RG. Predictions of the MSA + RG are in better agreement with experimental data than those of the MSA.

Figures 5, 6 and 7 present pressure-density isotherms at several compositions for carbon dioxide/*n*-butane, methane/

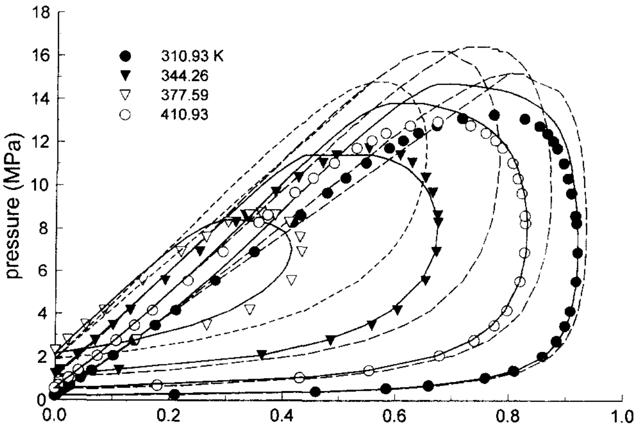

Figure 3. Pressure-composition envelopes for methane/*n*-butane mixtures.

(1) Experimental data (symbols); (2) mean-spherical approximation (dashed lines); and (3) mean-spherical approximation with renormalization corrections (solid lines) (experimental data from Sage et al. (1940)).

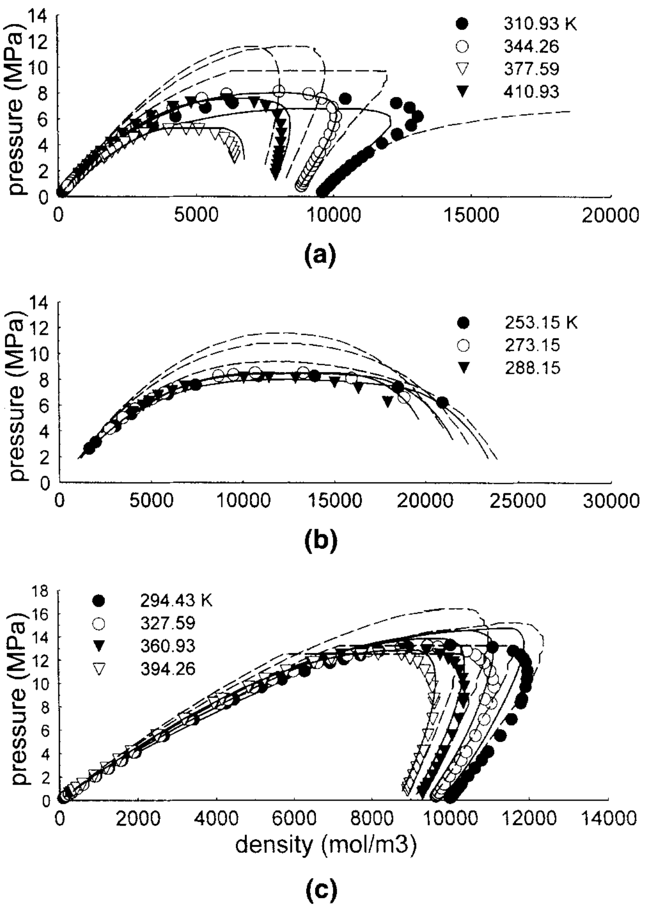

Figure 4. Phase densities for (a) carbon dioxide/ *n*-butane; (b) methane/carbon dioxide; and (c) methane/*n*-butane mixtures.

(1) Experimental data (symbols); (2) mean-spherical approximation (dashed lines); and (3) mean-spherical approximation with renormalization corrections (solid lines) (experimental data for carbon dioxide/*n*-butane are from Olds et al. (1949); for methane/carbon dioxide from Arai et al. (1971); and for methane/*n*-butane from Sage et al. (1940).

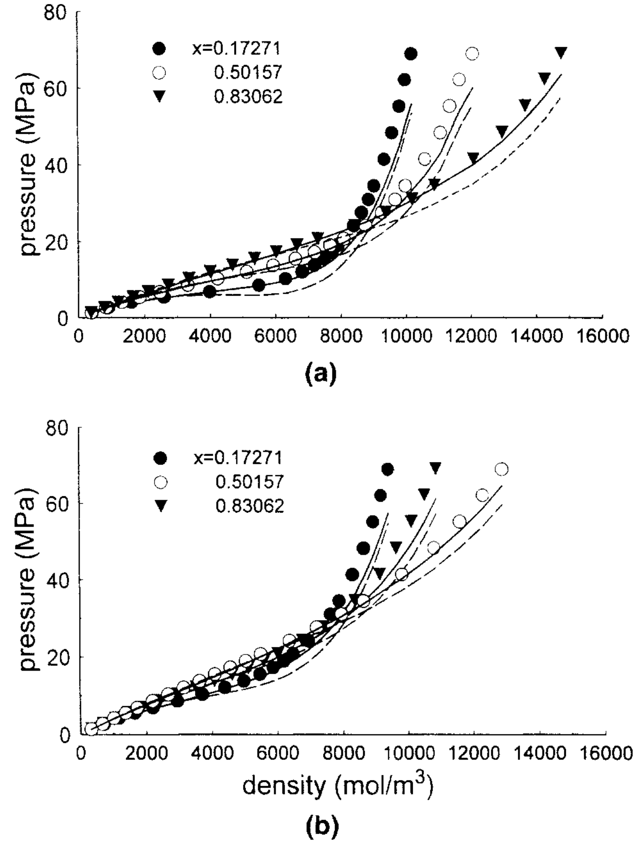

Figure 5. Equation of state for carbon dioxide/*n*-butane mixtures for (a) $T = 444.26$ K, and (b) $T = 510.93$ K.

(1) Experimental data (symbols); (2) mean-spherical approximation (dashed lines); and (3) mean-spherical approximation with renormalization corrections. The variable x is the mole fraction of carbon dioxide in the mixture (experimental data are from Olds et al. (1949)).

carbon dioxide, and methane/*n*-butane mixtures, respectively. For both theories, agreement with experiment is fairly good. At moderate to high densities both theories underestimate the pressure, but the MSA + RG results are in closer agreement with experiment than the MSA results. At low densities, the MSA is in better agreement with experiment; however, the difference in the predictions of the MSA and the MSA + RG at these conditions is small. This small difference could be due to inadequate subtraction of long-wavelength fluctuations from $f^{(s)}$ in Eq. 18, or perhaps to inadequacy of the recursion relations, Eqs. 23–28, at these conditions.

Conclusions

In an earlier article (Lue and Prausnitz, 1998), we proposed a method to extend the "global" renormalization-group corrections of White and coworkers for pure fluids to a wider region of densities and temperatures. In the present work, we extend our method to multicomponent fluids. To illustrate engineering applicability, we combine our method with the mean-spherical approximation to produce an equation of state for fluid mixtures valid near to and far from their critical points.

The MSA + RG results are in better agreement with experimental data than the MSA results. Far from the critical region of the fluid mixture, the predictions of the MSA and the MSA + RG coincide. Predictions of the MSA + RG can be adjusted by changing the parameter Δ_{12}. Decreasing Δ_{12} decreases the two-phase region.

The predictions of the MSA and the MSA + RG for the equation of state of the fluid mixture is fair. At moderate to high densities the MSA + RG yields better agreement with experiment than the MSA. However, at low densities, the MSA yields slightly better agreement with experiment. Overall, the MSA + RG results are better than those from the uncorrected MSA fit.

However, it is important to stress that modest agreement between theory and equation-of-state data is not primarily due to inadequacy of the renormalization corrections but, instead, to inadequacies in the base equation of state.

In this work, we use the MSA; however, in general, any model for the free energy can be used. The main direction for future improvement is first, to find a better reference equation valid at conditions not near critical; and second, to

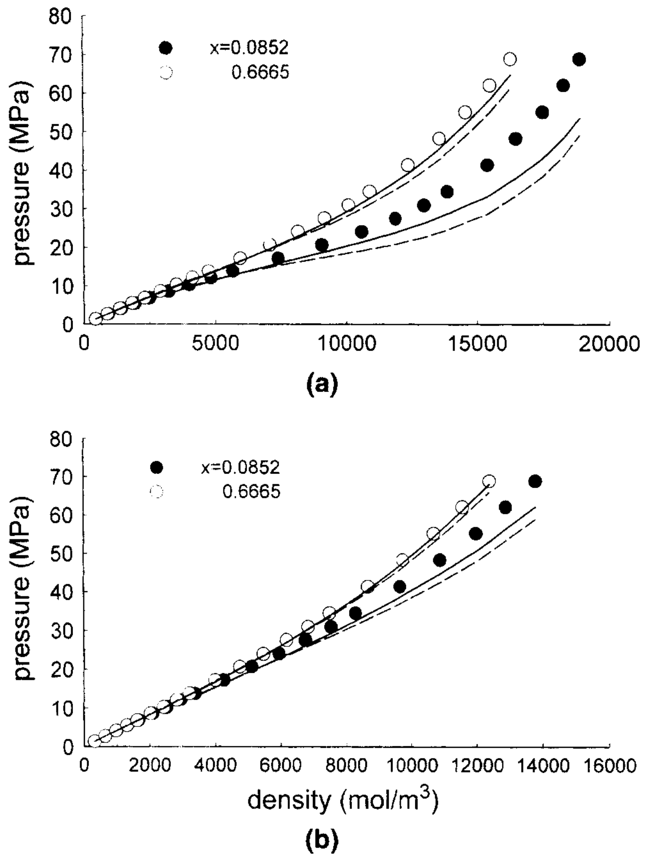

Figure 6. Equation of state for methane/carbon dioxide mixtures for (a) $T = 377.59$ K and (b) $T = 510.93$ K.

(1) Experimental data (symbols); (2) mean-spherical approximation (dashed lines); and (3) mean-spherical approximation with renormalization corrections (solid lines); the variable x is the mole fraction of methane in the mixture (experimental data are from Reamer et al. (1944)).

find a better way to subtract the long-wavelength approximation for the free energy contained in the reference equation.

The major advantage of our method is that it is not limited to type I fluids. In principle, it can be applied to any binary or higher multicomponent mixture, provided that a reliable equation of state exists for representing the properties of the fluid mixture at conditions remote from the critical region. Although we only examined vapor–liquid phase equilibria, our method can be used to study any type of fluid–phase coexistence behavior, including liquid–liquid phase equilibria.

The major shortcoming of our method is the numerical evaluation of the multidimensional integral in the recursion relation (Eq. 25). The dimension of the integral is equal to the number of components of the fluid. The more components in the fluid, the more computationally expensive the evaluation of the integral. Before this method can be of practical use for fluids with many components, it will be necessary to develop an efficient method to evaluate this multidimensional integral.

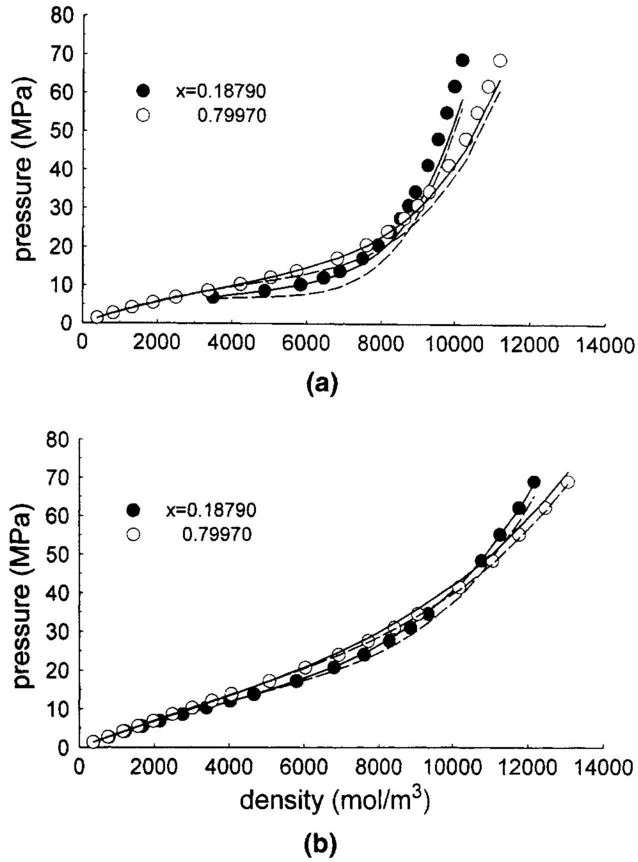

Figure 7. Equation of state for methane/*n*-butane mixtures for (a) $T = 444.26$ K, and (b) $T = 510.93$ K.

(1) Experimental data (symbols); (2) mean-spherical approximation (dashed lines); and (3) mean-spherical approximation with renormalization corrections (solid lines); the variable x is the mole fraction of methane in the mixture (experimental data are from Reamer et al. (1947)).

Acknowledgment

This work was supported by the Director, Office of Energy Research, Office of Basic Energy Sciences, Chemical Sciences Division of the U.S. Department of Energy under Contract No. DE-AC03-76SF0098. For additional support, the authors thank the Donors of the Petroleum Research Fund administered by the American Chemical Society. Leo Lue thanks the Miller Institute for Basic Research for a Postdoctoral Fellowship.

Notation

q = Fourier transform variable
Q = normalization factor
ν = generalized chemical potential
λ = reduced square-well width

Subscripts

k, s, t = molecule number
τ = species type

Literature Cited

Al-Sahhaf, T. A., A. J. Kidnay, and E. D. Sloan, "Liquid + Vapor Equilibria in the $N_2 + CO_2 + CH_4$ System," *Ind. Eng. Fund.*, **22**, 372 (1983).

Andersen, H. C., and D. Chandler, "Mode Expansion in Equilibrium Statistical Mechanics: I. General Theory and Application to the Classical Electron Gas," *J. Chem. Phys.*, **53**, 547 (1970).

Andersen, H. C., and D. Chandler, "Optimized Cluster Expansions for Classical Fluids. I. General Theory and Variational Formulation of the Mean Spherical Model and Hard Sphere Percus-Yevick Equations," *J. Chem. Phys.*, **57**, 1918 (1972).

Anisimov, M. A., E. E. Gorodetskii, V. D. Kulikov, and J. V. Sengers, "Crossover Between Vapor-Liquid and Consolute Critical Phenomena," *Phys. Rev. E*, **51**, 1199 (1995a).

Anisimov, M. A., E. E. Gorodetskii, V. D. Kulikov, A. A. Povodyrev, and J. V. Sengers, "A General Isomorphism Approach to Thermodynamic and Transport Properties of Binary Fluid Mixtures Near Critical Points," *Physica A*, **220**, 277 (1995b).

Anisimov, M. A., E. E. Gorodetskii, V. D. Kulikov, A. A. Povodyrev, and J. V. Sengers, "Erratum to: A General Isomorphism Approach to Thermodynamic and Transport Properties of Binary Fluid Mixtures Near Critical Points," *Physica A*, **223**, 272 (1996).

Arai, Y., G.-I. Kaminishi, and S. Saito, "The Experimental Determination of the P-V-T-*x* Relations for the Carbon Dioxide-Nitrogen and the Carbon Dioxide-Methane Systems," *J. Chem. Eng. Jpn.*, **4**, 113 (1971).

Battle, G., "Wavelet Refinement of the Wilson Recursion Formula," *Recent Advances in Wavelet Analysis*, L. L. Schumaker and G. Webb, eds., Academic Press, Boston, p. 87 (1994).

Bian, B. G., Y. R. Wang, J. Shi, E. S. Zho, and B. C. Y. Lu, "Simultaneous Determination of Vapor-Liquid-Equilibrium and Molar Volumes for Coexisting Phases Up to the Critical Temperature with a Static Method," *Fluid Phase Equil.*, **90**, 177 (1993).

Brown, T. S., V. G. Niesen, E. D. Sloan, and A. J. Kidnay, "Vapor-Liquid Equilibrium for the Binary Systems of Nitrogen, Carbon Dioxide, and *n*-Butane at Temperatures from 220 to 344 K," *Fluid Phase Equil.*, **53**, 7 (1989).

Carnahan, N. F., and K. E. Starling, "Equation of State for Nonattracting Rigid Spheres," *J. Chem. Phys.*, **51**, 635 (1969).

Chandler, D., and H. C. Andersen, "Mode Expansion in Equilibrium Statistical Mechanics. II. A Rapidly Convergent Theory of Ionic Solutions," *J. Chem. Phys.*, **54**, 26 (1971).

Chen, R. J. J., P. S. Chappelear, and R. Kobayashi, "Dew-Point Loci for Methane–*n*-Butane Binary System," *J. Chem. Eng. Data*, **19**, 53 (1974).

Chen, Z. Y., A. Abbaci, S. Tang, and J. V. Sengers, "Global Thermodynamic Behavior of Fluids in the Critical Region," *Phys. Rev. A*, **42**, 4470 (1990).

Cheng, H. Y., M. A. Anisimov, and J. V. Sengers, "Prediction of Thermodynamic and Transport Properties in the One-Phase Region of Methane + *n*-Hexane Mixtures Near Their Critical End Points," *Fluid Phase Equilib.*, **128**, 67 (1997).

Davalos, J., W. Anderson, R. Phelps, and A. J. Kidnay, "Liquid–Vapor Equilibria at 250.00 K for Systems Containing Methane, Ethane, and Carbon Dioxide," *J. Chem. Eng. Data*, **21**, 81 (1976).

Elliot, D. G., R. J. J. Chen, P. S. Chappelear, and R. Kobayashi, "Vapor-Liquid Equilibrium of Methane–*n*-Butane System at Low Temperatures and High Pressures," *J. Chem. Eng. Data*, **19**, 71 (1974).

Grover, M. K., "Critical Exponents for the X-Y Model," *Phys. Rev. B*, **6**, 3546 (1972).

Grover, M. K., L. P. Kadanoff, and F. J. Wegner, "Critical Exponents for the Heisenberg Model," *Phys. Rev. B*, **6**, 311 (1972).

Hansen, J. P., and I. R. McDonald, *Theory of Simple Fluids*, Academic Press, Boston (1986).

Hwang, S.-C., H. M. Lin, P. S. Chappelear, and R. Kobayashi, "Dew Point Study in the Vapor-Liquid Region of the Methane–Carbon Dioxide System," *J. Chem. Eng. Data*, **21**, 493 (1976).

Ivanchenko, Yu. M., and A. A. Lisyansky, *Physics of Critical Fluctuations*, Springer-Verlag, New York, p. 151 (1995).

Ivanchenko, Yu. M., and A. A. Lisyansky, "Generalized Renormalization Scheme in the Ginzburg-Landau-Wilson Model," *Phys. Rev. A*, **45**, 8525 (1992).

Ivanchenko, Yu. M., A. A. Lisyansky, and A. A. Filippov, "New Renormalization Procedure for Eliminating Redundant Operators," *J. Stat. Phys.*, **66**, 1139 (1992).

Jin, G. X., S. Tang, and J. V. Sengers, "Global Thermodynamic Behavior of Fluid Mixtures in the Critical Region," *Phys. Rev. E*, **47**, 388 (1993).

Kahre, L. C., "Low-Temperature K Data for Methane–*n*-Butane," *J. Chem. Eng. Data*, **19**, 67 (1974).

Kalra, H., T. R. Krishnan, and D. B. Robinson, "Equilibrium-Phase Properties of Carbon Dioxide–*n*-Butane and Nitrogen-Hydrogen Sulfide Systems at Subambient Temperatures," *J. Chem. Eng. Data*, **21**, 222 (1976).

Kiselev, S. B., "Universal Crossover Function for the Free Energy of Single-Component and Two-Component Fluids in the Critical Region," *High Temp.*, **28**, 42 (1990).

Kiselev, S. B., I. G. Kostyukova, and A. A. Povodyrev, "Universal Crossover Behavior of Fluids and Fluid Mixtures in the Critical Region," *Int. J. Thermophys.*, **12**, 877 (1991).

Kiselev, S. B., and J. V. Sengers, "An Improved Parametric Crossover Model for the Thermodynamic Properties of Fluids in the Critical Region," *Int. J. Thermophys.*, **14**, 1 (1993).

Kiselev, S. B., and I. G. Kostyukova, "Spinodal and Kinetic Boundary of Metastable Region," *J. Chem. Phys.*, **98**, 6455 (1993).

Kiselev, S. B., "Prediction of the Thermodynamic Properties and the Phase Behavior of Binary Mixtures in the Extended Critical Region," *Fluid Phase Equil.*, **128**, 1 (1997).

Kleinrahm, R., and W. Wagner, "Measurement and Correlation of the Equilibrium Liquid and Vapour Densities and the Vapour Pressure Along the Coexistence Curve of Methane," *J. Chem. Thermody.*, **18**, 739 (1986).

Leung, S. S., and R. B. Griffiths, "Thermodynamic Properties Near the Liquid-Vapor Critical Line in Mixtures of He^3 and He^4," *Phys. Rev. A*, **8**, 2673 (1973).

Lue, L., and J. M. Prausnitz, "Renormalization-Group Corrections to and an Approximation Free-Energy Model for Simple Fluids," *J. Chem. Phys.*, **108**, 5529 (1998).

Ma, S.-K., *Modern Theory of Critical Phenomena*, Benjamin/Cummings, Reading, MA, p. 229 (1976).

Mansoori, G. A., N. F. Carnahan, K. E. Starling, and T. W. Leland, Jr., "Equilibrium Thermodynamic Properties of the Mixtures of Hard Spheres," *J. Chem. Phys*, **54**, 1523 (1971).

Meroni, A., A. Parola, and L. Reatto, "Differential Approach to the Theory of Fluids," *Phys. Rev. A*, **42**, 6104 (1990).

Meroni, A., L. Reatto, and M. Tau, "Differential Approach to the Theory of Fluids in the Presence of Two- and Three-Body Potentials and Study of the Critical Point of Krypton," *Mol. Phys.*, **80**, 977 (1993).

Mraw, S. C., S. C. Hwang, and R. Kobayashi, "Vapor-Liquid Equilibrium of the CH_4–CO_2 System at Low Temperatures," *J. Chem. Eng. Data*, **23**, 135 (1978).

Nagahama, K., H. Konishi, D. Hoshino, and M. Hirata, "Binary Vapor-Liquid Equilibria of Carbon Dioxide-Light Hydrocarbons at Low Temperatures," *J. Chem. Eng. Jpn.*, **7**, 323 (1974).

Negele, J. W., and H. Orland, *Quantum Many-Particle Systems*, Addison-Wesley, Redwood City, CA, p. 204 (1988).

Olds, R. H., H. H. Reamer, B. H. Sage, and W. N. Lacey, "Phase Equilibria in Hydrocarbon Systems: The *n*-Butane–Carbon Dioxide System," *Ind. Eng. Chem.*, **41**, 475 (1949).

Parola, A., and L. Reatto, "Microscopic Approach to Critical Phenomena in Binary Fluids," *Phys. Rev. A*, **44**, 6600 (1991).

Parola, A., and L. Reatto, "The Order Parameter and Crossovers at Critical Points of Binary Mixtures," *J. Phys. Cond. Mater.*, **5**(S34B), B165 (1993).

Parola, A., and L. Reatto, "Liquid-State Theory for Critical Phenomena," *Phys. Rev. Lett.*, **53**, 2417 (1984).

Parola, A., and L. Reatto, "Hierarchical Reference Theory of Fluids and the Critical Point," *Phys. Rev. A*, **31**, 3309 (1985).

Povodyrev, A. A., G. X. Jin, S. S. Kiselev, and J. V. Sengers, "Crossover Equation of State for the Thermodynamic Properties of Mixtures of Methane and Ethane in the Critical Region," *Int. J. Thermophys.*, **17**, 909 (1996).

Pozo de Fernandez, M. E., J. A. Zollweg, and W. B. Streett, "Vapor-Liquid Equilibrium in the Binary System Carbon Dioxide + *n*-Butane," *J. Chem. Eng. Data*, **34**, 324 (1989).

Reamer, H. H., R. H. Olds, B. H. Sage, and W. N. Lacey, "Phase Equilibria in Hydrocarbon Systems: Methane-Carbon Dioxide in the Gaseous Region," *Ind. Eng. Chem.*, **36**, 88 (1944).

Reamer, H. H., K. J. Korpi, B. H. Sage, and W. N. Lacey, "Phase Equilibria in Hydrocarbon Systems: Volumetric Behavior of Methane–*n*-Butane System at Higher Pressures," *Ind. Eng. Chem.*, **39**, 206 (1947).

Roberts, L. R., R. H. Wang, A. Azarnoosh, and J. J. McKetta, "Methane–*n*-Butane System in the Two-Phase Region," *J. Chem. Eng. Data*, **7**, 484 (1962).

Sage, B. H., R. L. Hicks, and W. N. Lacey, "Phase Equilibria in Hydrocarbon Systems: The Methane–*n*-Butane System in the Two-Phase Region," *Ind. Eng. Chem.*, **34**(8), 1085 (1940).

Salvino, L. W., and J. A. White, "Calculation of Density Fluctuation Contributions to Thermodynamic Properties of Simple Fluids," *J. Chem. Phys.*, **96**, 4559 (1992).

Sengers, J. M. H. L., "Thermodynamics of Solutions Near the Solvent's Critical Point," *Supercritical Fluid Technology Reviews in Modern Theory and Applications*, T. J. Bruno and J. F. Ely, eds., CRC Press, Boca Raton, FL, p. 1 (1991).

Shibata, S. K., and S. I. Sandler, "High-Pressure Vapor-Liquid Equilibria Involving Mixtures of Nitrogen, Carbon Dioxide, and *n*-Butane," *J. Chem. Eng. Data*, **34**, 291 (1989).

Somait, F. A., and A. J. Kidnay, "Liquid-Vapor Equilibria at 270.00 K for Systems Containing Nitrogen, Methane, and Carbon Dioxide," *J. Chem. Eng. Data*, **23**, 301 (1983).

Tang, Y., and B. C.-Y. Lu, "An Analytical Analysis of the Square-Well Fluid Behaviors," *J. Chem. Phys.*, **100**, 6665 (1994).

Tang, Y., and B. C.-Y. Lu, "Analytical Solution of the Ornstein-Zernike Equation for Mixtures," *Mol. Phys.*, **84**, 89 (1995).

Traub, P., and K. Stephan, "High Pressure Phase Equilibria of the System CO$_2$-Water-Acetone Measured with a New Apparatus," *Chem. Eng. Sci.*, **45**, 751 (1990).

Vargaftik, N. B., *Tables on the Thermophysical Properties of Liquids and Gases*, Hemisphere, Washington, DC, p. 167 (1975).

Weber, L. A., "Simple Apparatus for Vapor-Liquid Equilibrium Measurements with Data for the Binary Systems of Carbon Dioxide with *n*-Butane and Isobutane," *J. Chem. Eng. Data*, **34**, 171 (1989).

Weeks, J. D., D. Chandler, and H. C. Andersen, "Role of Repulsive Forces in Determining the Equilibrium Structure of Simple Liquids," *J. Chem. Phys.*, **54**, 5237 (1971).

White, J. A., and S. Zhang, "Renormalization Group Theory for Fluids," *J. Chem. Phys.*, **99**, 2012 (1993).

White, J. A., and S. Zhang, "Renormalization Theory of Nonuniversal Thermal Properties of Fluids," *J. Chem. Phys.*, **103**, 1922 (1995).

White, J. A., and S. Zhang, "Renormalization Group Theory for Fluids to Greater Density Distances from the Critical Point," Symp. on Thermophysical Properties, Boulder, CO (1997).

Wilson, K. G., "Renormalization Group and Critical Phenomena: I. Renormalization Group and the Kadanoff Scaling Picture," *Phys. Rev. B*, **4**, 3174 (1971a).

Wilson, K. G., "Renormalization Group and Critical Phenomena: II. Phase-Space Cell Analysis of Critical Behavior," *Phys. Rev. B*, **4**, 3184 (1971b).

Wilson, K. G., and M. E. Fisher, "Critical Exponents in 3.99 Dimensions," *Phys. Rev. Lett.*, **28**, 240 (1972).

Xu, N., J. Dong, Y. Wang, and J. Shi, "High Pressure Vapor Liquid Equilibria at 293 K for Systems Containing Nitrogen, Methane, and Carbon Dioxide," *Fluid Phase Equil.*, **81**, 175 (1992).

Younglove, B. A., and J. F. Ely, "Thermophysical Properties of Fluids: II. Methane, Ethane, Propane, Isobutane, and Normal Butane," *J. Phys. Chem. Ref. Data*, **16**, 577 (1987).

Appendix: Derivation of Recursion Relations

To perform the integration in Eq. 22, we first need to define precisely what is meant by a smooth density profile at length scale L. To do this, each density distribution, ρ_α, is expanded in terms of the basis functions, $\psi_\alpha^{(ml)}(r)$. These basis functions are constructed from translations and dilations of a single function, ψ_α. That is,

$$\psi_\alpha^{(ml)}(r) = \psi_\alpha\left(\frac{r}{2^l L} - m\right), \tag{A1}$$

where m and l are integers. We require that the functions ψ_α satisfy the following properties (Battle, 1994):

1. ψ_α is nearly zero outside the cube

$$\mathcal{C} = [0,1]\times[0,1]\times[0,1].$$

2. The functions $\psi_\alpha^{(ml)}$ are orthogonal with respect to the Sobolev norm,

$$\int d^3r \nabla\psi_\alpha^{(ml)}(r)\cdot\nabla\psi_\gamma^{(m'l')}(r) = (2^l L)\Delta_{\alpha\gamma}\,\delta_{ll'}\,\delta_{mm'}, \tag{A2}$$

where δ is the Kronecker delta, and $\Delta_{\alpha\gamma}$ is a normalization factor that depends on the particular definition of the functions $\psi_\alpha^{(ml)}$.

3. $|\psi_\alpha(r)| \approx 1$ in the cube $\mathcal{C}$.

4. $\int_{\mathcal{C}} d^3r\psi_\alpha(r) = 0$, where the subscript $\mathcal{C}$ on the integral sign means that the domain of integration is the cube $\mathcal{C}$.

Any function that has a finite Sobolev norm can be represented in terms of these basis functions. For example, the density distribution, $\rho_\alpha(r)$, can be expressed as

$$\rho_\alpha(r) = \sum_{m=-\infty}^{\infty}\sum_{l=-\infty}^{\infty} P_\alpha^{(ml)}\psi_\alpha^{(ml)}(r). \tag{A3}$$

If $\rho_\alpha^{(l)}$ is a density distribution that is smooth on length scale $2^l L$, the density can be expressed as (Battle, 1994)

$$\rho_\alpha^{(l)}(r) = \sum_m \sum_{l'\geq l} P_\alpha^{(ml')}\psi_\alpha^{(ml')}(r). \tag{A4}$$

From this expansion, we find that the density at length scale $2^{l-1}L$ can be related to the density at length scale $2^l L$ by

$$\rho_\alpha^{(l-1)}(r) = \rho_\alpha^{(l)}(r) + \sum_m P_\alpha^{(ml)}\psi_\alpha^{(ml)}(r). \tag{A5}$$

The Hamiltonian at length scale $2^{l-1}L$, $\mathcal{H}^{(l-1)}$ can be determined from the Hamiltonian at length scale $2^l L$, $\mathcal{H}^{(l)}$ by integrating over the expansion coefficients $P_\alpha^{(ml)}$

$$\exp\{-\beta\mathcal{H}^{(l)}[\boldsymbol{\rho}^{(l)}]\} = \frac{1}{\mathfrak{N}}\int\prod_{\tau m} dP_\tau^{(ml)}\exp\{-\beta\mathcal{H}^{(l-1)}[\boldsymbol{\rho}^{(l-1)}]\}, \tag{A6}$$

where $\mathfrak{N}$ is a normalization constant to be discussed later, and the Hamiltonian is defined as

$$\mathcal{H}^{(l)}[\boldsymbol{\rho}^{(l)}] = \sum_{\alpha\gamma}\frac{a_{\alpha\gamma}\zeta_{\alpha\gamma}^2}{2}\int d^3r\nabla\rho_\alpha^{(l)}(r)\cdot\nabla\rho_\gamma^{(l)}(r) + \int d^3r f^{(1)}(\boldsymbol{\rho}^{(l)}(r)). \tag{A7}$$

Substituting Eq. A5 into the gradient term of the Hamiltonian, we find

$$\begin{aligned}\int d^3r\nabla\rho_\alpha^{(l-1)}(r)\cdot\nabla\rho_\gamma^{(l-1)}(r) &= \int d^3r\nabla\rho_\alpha^{(l)}(r)\cdot\nabla\rho_\gamma^{(l)}(r)\\ &\quad + \sum_m \int d^3r P_\gamma^{(ml)}\nabla\rho_\alpha^{(l-1)}(r)\cdot\nabla\psi^{(ml)}(r)\\ &\quad + \sum_{mm'}\int d^3r P_\alpha^{(ml)}P_\gamma^{(m'l)}\nabla\psi^{(ml)}(r)\cdot\nabla\psi^{(m'l)}(r)\\ &= \int d^3r\nabla\rho_\alpha^{(l)}(r)\cdot\nabla\rho_\gamma^{(l)}(r) + (2^l L)\sum_m P_\alpha^{(ml)}P_\gamma^{(ml)}\Delta_{\alpha\gamma},\end{aligned} \tag{A8}$$

where we have made use of Eq. A2.

Substituting Eq. A5 into the first term of the Hamiltonian, we find

$$\int d^3 r f^{(l-1)}(\boldsymbol{\rho}^{(l-1)}(r))$$

$$= \int d^3 r f^{(l-1)}\left(\boldsymbol{\rho}^{(l)}(r) + \sum_m \boldsymbol{P}^{(ml)}\boldsymbol{\psi}^{(ml)}(r)\right). \quad (A9)$$

Requirement (1) states that the function $\psi_\alpha(r)$ is approximately equal to zero outside the cube $\mathcal{C}$. Combined with Eq. A1, this implies that the functions $\psi_\alpha^{(ml)}(r)$ are approximately equal to zero outside the cube

$$\mathcal{C}^{(ml)} = \left[2^l L m_1, 2^l L(m_1+1)\right] \times \left[2^l L m_2, 2^l L(m_2+1)\right]$$
$$\times \left[2^l L m_3, 2^l L(m_3+1)\right].$$

Therefore, the integral can be divided into a sum of integrals over each cube $\mathcal{C}^{(ml)}$. This yields

$$\int d^3 r f^{(l-1)}[\boldsymbol{\rho}^{(l-1)}(r)]$$

$$= \sum_m \int_{\text{box } m} d^3 r f^{(l-1)}[\rho^{(l)}(r) + \boldsymbol{P}^{(ml)} \cdot \boldsymbol{\psi}^{(ml)}(r)].$$

Requirements (3) and (4) imply that over half of the cube $\mathcal{C}^{(ml)}$, $\psi_\alpha^{ml}(r) \approx 1$, while in the other half $\psi_\alpha^{ml}(r) \approx -1$. With this we find that

$$\int d^3 r f^{(l-1)}(\boldsymbol{\rho}^{(l-1)}(r))$$

$$= \frac{(2^l L)^3}{2} \sum_m \left[f^{(l-1)}(\boldsymbol{\rho}^{(l)}(2^l Lm) + \boldsymbol{P}^{(ml)})\right.$$
$$\left. + f^{(l-1)}(\boldsymbol{\rho}^{(l)}(2^l Lm) - \boldsymbol{P}^{(ml)})\right]. \quad (A10)$$

Introducing Eqs. A8 and A10 into Eq. A6, we find

$$\{-\beta\mathcal{H}^{(l)}[\boldsymbol{\rho}^{(l)}]\} = \frac{1}{\mathfrak{N}} \int \prod_{\tau m} dP_{\tau m} \exp\{-\beta\mathcal{H}^{(l-1)}[\boldsymbol{\rho}^{(l-1)}]\}$$

$$= \exp\left\{-\sum_{\alpha\gamma} \frac{a_{\alpha\gamma}\zeta_{\alpha\gamma}^2}{2} \int d^3 r \nabla\rho_\alpha^{(l)}(r) \cdot \nabla\rho_\gamma^{(l)}(r)\right\} \times \frac{1}{\mathfrak{N}} \int \prod_{m'\tau} dP_\tau^{(m'l)}$$

$$\times \exp\left\{-\frac{(2^l L)\beta}{2} \sum_{\alpha\gamma} a_{\alpha\gamma}\zeta_{\alpha\gamma}^2 \sum_m P_\alpha^{(ml)} P_\gamma^{(ml)} \Delta_{\alpha\gamma} - \frac{(2^l L)^3 \beta}{2}\right.$$

$$\left.\times \sum_m \left[f^{(l-1)}(\boldsymbol{\rho}^{(l)})(2^l Lm) + \boldsymbol{P}^{(ml)} + f^{(l-1)}(\boldsymbol{\rho}^{(l)}(2^l Lm) - \boldsymbol{P}^{(ml)})\right]\right\}$$

$$= \exp\left\{-\sum_{\alpha\gamma} \frac{a_{\alpha\gamma}\zeta_{\alpha\gamma}^2}{2} \int d^3 r \nabla\rho_\alpha^{(l)}(r) \cdot \nabla\rho_\gamma^{(l)}(r)\right\}$$

$$\times \frac{1}{\mathfrak{N}} \prod_m \left[\int \prod_\tau dP_\tau^{(ml)} \exp\left\{-(2^l L)^3 \beta \left[\sum_{\alpha\gamma} \frac{a_{\alpha\gamma}\Delta_{\alpha\gamma}}{2} \left(\frac{\zeta_{\alpha\gamma}}{2^l L}\right)^2\right.\right.\right.$$

$$\left.\left.\left.\times P_\alpha^{(ml)} P_\gamma^{(ml)} + \frac{1}{2}\left[f^{(l-1)}(\boldsymbol{\rho}^{(l)}(2^l Lm) + \boldsymbol{P}^{(ml)})\right.\right.\right.\right.$$

$$\left.\left.\left.\left. - f^{(l-1)}(\boldsymbol{\rho}^{(l)}(2^l Lm) - \boldsymbol{P}^{(ml)})\right]\right]\right\}\right] - \beta\mathcal{H}^{(l)}[\boldsymbol{\rho}^{(l)}]$$

$$= -\sum_{\alpha\gamma} \frac{a_{\alpha\gamma}\zeta_{\alpha\gamma}^2}{2} \int d^3 r \nabla\rho_\alpha^{(l)}(r) \cdot \nabla\rho_\gamma^{(l)}(r)$$

$$-\sum_m \left[f^{(l-1)}[\boldsymbol{\rho}^{(l)}(2^l Lm)] + \ln I'[\boldsymbol{\rho}^{(l)}(2^l Lm)]\right] \quad (A11)$$

where

$$I'(\rho) = \frac{1}{\mathfrak{N}} \int \prod_\tau dP_\tau \exp\left\{-(2^l L)^3 \beta \left[\sum_{\alpha\gamma} \frac{a_{\alpha\gamma}\Delta_{\alpha\gamma}}{2} \left(\frac{\zeta_{\alpha\gamma}}{2^l L}\right)^2 P_\alpha P_\gamma\right.\right.$$

$$\left.\left. + \frac{1}{2}\left[f^{(l-1)}(\boldsymbol{\rho} + \boldsymbol{P}) + f^{(l-1)}(\bar{\rho} - \boldsymbol{P})\right]\right] - f^{(l-1)}(\boldsymbol{\rho})\right\}.$$

$$(A12)$$

Because the density profiles, $\rho_\alpha^{(l)}$, are fairly constant on length scales less than $2^l L$, the system can be considered as being divided into cubes of width $2^l L$. Integrals can be considered as sums with differential volume element $d^3 r = (2^l L)^3$, and we can make the replacement $\Sigma_m (2^l L)^3 \to \int d^3 r$. Performing this substitution yields

$$-\beta\mathcal{H}^{(l)}[\rho^{(l)}] = -\sum_{\alpha\gamma} \frac{a_{\alpha\gamma}\zeta_{\alpha\gamma}^2}{2} \int d^3 r \nabla\rho_\alpha^{(l)}(r) \cdot \nabla\rho_\gamma^{(l)}(r)$$

$$-\int d^3 r \left[f^{(l-1)}(\boldsymbol{\rho}^{(l)}(r)) + \frac{1}{(2^l L)^3} \ln I'(\boldsymbol{\rho}^{(l)}(r))\right]. \quad (A13)$$

Comparing this expression with the definition of the Hamiltonian (see Eq. A7), we find

$$f^{(l)}(\boldsymbol{\rho}) = f^{(l-1)}(\boldsymbol{\rho}) + \frac{k_B T}{(2^l L)^3} \ln I'(\boldsymbol{\rho}). \quad (A14)$$

To determine the $\mathfrak{N}$, we use the procedure of White and coworkers. If perturbation potential $v_{\alpha\gamma}^{(l)}(r)$ is equal to zero, then the free energy should be fully accounted for by the function $f^{(s)}$. The renormalization procedure should therefore leave the free energy unaffected. This implies that

$$\mathfrak{N} = \int \prod_\tau dP_\tau \exp\left\{-(2^l L)^3 \beta \left[\sum_{\alpha\gamma} \frac{a_{\alpha\gamma}}{2} P_\alpha P_\gamma\right.\right.$$

$$\left.\left. + \frac{1}{2}\left[f^{(l-1)}(\boldsymbol{\rho} + \boldsymbol{P}) + f^{(l-1)}(\boldsymbol{\rho} - \boldsymbol{P})\right]\right] - f^{(l-1)}(\boldsymbol{\rho})\right\}.$$

$$(A15)$$

This process results in the recursion relations defined in Eqs. 23–28 to determine the long-wavelength fluctuation corrections to the free energy of a fluid.

Manuscript received Sept. 8, 1997, and revision received Mar. 18, 1998.